Strong Absorption of Hadrons with Hidden and Open Strangeness in Nuclear Matter

J. Adamczewski-Musch,[4] O. Arnold,[10,9] E. T. Atomssa,[16] C. Behnke,[8] A. Belounnas,[16] A. Belyaev,[7] J. C. Berger-Chen,[10,9]
J. Biernat,[3] A. Blanco,[1] C. Blume,[8] M. Böhmer,[10] S. Chernenko,[7,*] L. Chlad,[17] P. Chudoba,[17] I. Ciepał,[2] C. Deveaux,[11]
D. Dittert,[5] J. Dreyer,[6] E. Epple,[10,9] L. Fabbietti,[10,9] O. Fateev,[7] P. Fonte,[1,a] C. Franco,[1] J. Friese,[10] I. Fröhlich,[8]
T. Galatyuk,[5,4] J. A. Garzón,[18] R. Gernhäuser,[10] M. Golubeva,[12] R. Greifenhagen,[6,c] F. Guber,[12] M. Gumberidze,[4,b]
S. Harabasz,[5,3] T. Heinz,[4] T. Hennino,[16] C. Höhne,[11,4] R. Holzmann,[4] A. Ierusalimov,[7] A. Ivashkin,[12] B. Kämpfer,[6,c]
B. Kardan,[8] I. Koenig,[4] W. Koenig,[4] B. W. Kolb,[4] G. Korcyl,[3] G. Kornakov,[5] F. Kornas,[5] R. Kotte,[6] J. Kuboś,[2] A. Kugler,[17]
T. Kunz,[10] A. Kurepin,[12] A. Kurilkin,[7] P. Kurilkin,[7] V. Ladygin,[7] R. Lalik,[3] K. Lapidus,[10,9] A. Lebedev,[13] S. Linev,[4]
L. Lopes,[1] M. Lorenz,[8] T. Mahmoud,[11] L. Maier,[10] A. Malige,[3] J. Markert,[4] S. Maurus,[10] V. Metag,[11] J. Michel,[8]
D. M. Mihaylov,[10,9] V. Mikhaylov,[17] S. Morozov,[12,14] C. Müntz,[8] R. Münzer,[10,9] L. Naumann,[6] K. Nowakowski,[3]
Y. Parpottas,[15,d] V. Pechenov,[4] O. Pechenova,[4] O. Petukhov,[12] J. Pietraszko,[4] A. P. Prozorov,[17] W. Przygoda,[3] B. Ramstein,[16]
N. Rathod,[3] A. Reshetin,[12] P. Rodriguez-Ramos,[17] A. Rost,[5] A. Sadovsky,[12] P. Salabura,[3] T. Scheib,[8] K. Schmidt-Sommerfeld,[10]
H. Schuldes,[8] E. Schwab,[4] F. Scozzi,[5,16] F. Seck,[5] P. Sellheim,[8] J. Siebenson,[10] L. Silva,[1] J. Smyrski,[3]
S. Spataro,[20] S. Spies,[8] H. Ströbele,[8] J. Stroth,[8,4,e] P. Strzempek,[3] C. Sturm,[4] O. Svoboda,[17] M. Szala,[8] P. Tlusty,[17]
M. Traxler,[4] H. Tsertos,[15] C. Ungethüm,[5] O. Vázquez Doce,[9,8] V. Wagner,[17] C. Wendisch,[4] M. G. Wiebusch,[8] J. Wirth,[10,9]
D. Wójcik,[19] Y. Zanevsky,[7,*] and P. Zumbruch[4]

(HADES Collaboration)

C. Curceanu,[21] K. Piscicchia,[22,21] and A. Scordo[21]
[1]*LIP-Laboratório de Instrumentação e Física Experimental de Partículas, 3004-516 Coimbra, Portugal*
[2]*Institute of Nuclear Physics, Polish Academy of Sciences, 31342 Kraków, Poland*
[3]*Smoluchowski Institute of Physics, Jagiellonian University of Cracow, 30-059 Kraków, Poland*
[4]*GSI Helmholtzzentrum für Schwerionenforschung GmbH, 64291 Darmstadt, Germany*
[5]*Technische Universität Darmstadt, 64289 Darmstadt, Germany*
[6]*Institut für Strahlenphysik, Helmholtz-Zentrum Dresden-Rossendorf, 01314 Dresden, Germany*
[7]*Joint Institute of Nuclear Research, 141980 Dubna, Russia*
[8]*Institut für Kernphysik, Goethe-Universität, 60438 Frankfurt, Germany*
[9]*Excellence Cluster "Origin and Structure of the Universe," 85748 Garching, Germany*
[10]*Physik Department E62, Technische Universität München, 85748 Garching, Germany*
[11]*II.Physikalisches Institut, Justus Liebig Universität Giessen, 35392 Giessen, Germany*
[12]*Institute for Nuclear Research, Russian Academy of Science, 117312 Moscow, Russia*
[13]*Institute of Theoretical and Experimental Physics, 117218 Moscow, Russia*
[14]*National Research Nuclear University MEPhI (Moscow Engineering Physics Institute),*
115409 Moscow, Russia
[15]*Department of Physics, University of Cyprus, 1678 Nicosia, Cyprus*
[16]*Institut de Physique Nucléaire, CNRS-IN2P3, Univ. Paris-Sud, Université Paris-Saclay,*
F-91406 Orsay Cedex, France
[17]*Nuclear Physics Institute, The Czech Academy of Sciences, 25068 Rez, Czech Republic*
[18]*LabCAF. F. Física, Univ. de Santiago de Compostela, 15706 Santiago de Compostela, Spain*
[19]*Uniwersytet Warszawski - Instytut Fizyki Doświadczalnej, 02-093 Warszawa, Poland*
[20]*Dipartimento di Fisica and INFN, Università di Torino, 10125 Torino, Italy*
[21]*INFN, Laboratori Nazionali di Frascati, 00044 Frascati, Italy*
[22]*CENTRO FERMI - Museo Storico della Fisica e Centro Studi e Ricerche "Enrico Fermi", 00184 Rome, Italy*

(Received 18 December 2018; revised manuscript received 29 April 2019; published 9 July 2019)

We present the first observation of K^- and ϕ absorption within nuclear matter by means of π^--induced reactions on C and W targets at an incident beam momentum of 1.7 GeV/c studied with HADES at SIS18/GSI. The double ratio $(K^-/K^+)_{\mathrm{W}}/(K^-/K^+)_{\mathrm{C}}$ is found to be $0.319 \pm 0.009(\mathrm{stat})^{+0.014}_{-0.012}(\mathrm{syst})$ indicating a larger absorption of K^- in heavier targets as compared to lighter ones. The measured ϕ/K^- ratios in $\pi^- + \mathrm{C}$ and $\pi^- + \mathrm{W}$ reactions within the HADES acceptance are found to be equal to $0.55 \pm 0.04(\mathrm{stat})^{+0.06}_{-0.07}(\mathrm{syst})$ and to $0.63 \pm 0.06(\mathrm{stat})^{+0.11}_{-0.11}(\mathrm{syst})$, respectively. The similar ratios measured in the two different reactions demonstrate for the first time experimentally that the dynamics of the ϕ meson in nuclear medium is strongly coupled to the K^- dynamics. The large difference in the ϕ production off C and W nuclei is discussed in terms of a strong ϕN in-medium coupling. These results are relevant for the description of heavy-ion collisions and the structure of neutron stars.

DOI: 10.1103/PhysRevLett.123.022002

Hadron-hadron interactions are studied to understand in detail low energy QCD [1,2] in vacuum, but also in nuclear matter at finite temperature and density [3]. In this context, absorption processes play an important role but are often neglected in the computation of the equation of state (EOS).

The antikaon-nucleon interaction is particularly interesting because the large $\bar{K}N$ coupling to the $\Lambda(1405)$ resonance [4,5] leads to absorption processes for the $\bar{K}N$ and $\bar{K}NN$ states [6–9]. Within nuclear matter, possible modifications of the $\Lambda(1405)$ spectral function will also affect the $\bar{K}$ spectral function [3,10]. So far, scattering experiments, kaonic atom data [11–14], and recent evidence for the existence of ppK^- bound states [15] demonstrate that the $\bar{K}N$ interaction is attractive, but an accurate measurement of absorption in (heavy) nuclei is still missing.

Due to the attractive nature of the $\bar{K}N$ interaction, hypotheses have been made in the past about the presence of antikaons within neutron stars (NS) [16,17]. This scenario neglects the imaginary part of the $\bar{K}N$ interaction, which leads to absorption processes and thus to hyperon production. A quantitative determination of the $\bar{K}$ absorption is therefore crucial to provide a more realistic EOS of dense matter and scenarios for NS and NS merger [18,19].

The behavior of ϕ mesons in the nuclear medium is also complex and has been debated for decades. It is strongly coupled with kaons and antikaons evident from the branching ratio $\phi \to \bar{K}K$ ($BR \approx 83\%$ [11]). The ϕ spectral functions have been computed using chiral effective field theories [20,21]. The results predict broadening of the meson width (40–50 MeV) due to in-medium modifications of kaon loop and direct ϕN interactions.

So far, in the interpretation of the ultrarelativistic heavy-ion collision data [22,23], the ϕN cross sections are assumed to be small [24], mainly due to OZI suppression [25] hindering processes with disconnected quark lines. On the contrary, measurements of the modification of the ϕ production rates in proton- and photon-induced reactions do suggest a rather sizable ϕN interaction cross section [26–28]. These data are, however, interpreted in a rather model-dependent way [29,30] implying the contribution of secondary processes, in-medium propagation, and initial and final state interactions.

If one considers the in-medium ϕ properties in the context of NS, the ϕN coupling strength plays a decisive role in the description of hyperon-hyperon interactions [31]. This means that a direct evidence of a significant ϕN coupling would lead to more realistic EOS of dense nuclear matter with hyperon content, in heavy ion collisions, but possibly also in NS [32].

In this Letter, we present the first measurement of the direct coupling of the ϕ to antikaon properties within nuclear matter, showing that for both mesons a strong absorption is observed when comparing $\pi^- + \mathrm{W}$ to $\pi^- + \mathrm{C}$ reactions at a π^- momentum of 1.7 GeV$/c$. The employment of pion-induced reactions is motivated by the fact that the latter are superior to the previously studied proton- and photon-induced reactions. Due to the large πN inelastic cross section, hadron production occurs close to the upstream surface of the nucleus [33,34], leading on average to a longer path of the produced hadrons inside nuclear matter. Because of the much lower production cross section of the mesons in proton-induced reactions, secondary processes are non-negligible, causing shorter path lengths, just as in photon-induced reactions where the incident photons penetrate deeply into the nucleus.

The experiment was performed with the High Acceptance DiElectron Spectrometer (HADES) at the SIS18 at GSI Helmholtzzentrum für Schwerionenforschung in Darmstadt, Germany. HADES [35] is a charged-particle detector consisting of a six-coiled toroidal magnet surrounding the beam axis with six identical detection sections. It features polar acceptance between 18° and 85° with an almost full azimuthal coverage. Each sector is equipped with a ring-imaging Cherenkov (RICH) detector followed by mini-drift chambers (MDCs), two in front of and two behind the magnetic field, as well as two detectors for time-of-flight measurements, a scintillator hodoscope (TOF), and resistive plate chamber (RPC), in combination with the target-T0 detector. In the following, the TOF-RPC system is referred to as multiplicity electron trigger array (META). Hadron identification is based on time of flight and on specific energy loss (dE/dx) in the MDC tracking detectors.

A secondary beam of negatively charged pions with a rate of $\approx 3 \times 10^5 \pi^-/\mathrm{s}$ and a momentum of 1.7 GeV$/c$ was incident on carbon and tungsten targets each composed of three segments with a thickness of 3×7.2 mm and 3×2.4 mm, respectively. The measurements on the two targets were carried out in separate runs. In order to measure the momentum of the secondary pion beam with a precision of $\approx 0.3\%(\sigma)$, the CERBEROS tracking system [36] was employed. The first level trigger (LVL1) required a signal in the target-T0 detector and a minimum charged particle multiplicity $M \geq 2$ in the META system. A total of 1.3×10^8 and 1.7×10^8 events were collected for $\pi^- + \mathrm{C}$ and $\pi^- + \mathrm{W}$ collisions, respectively.

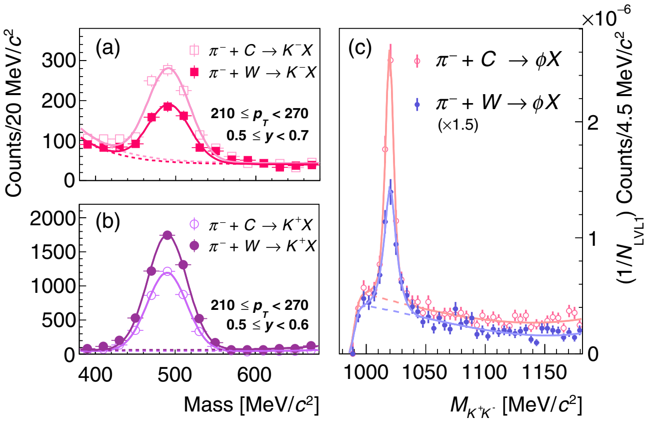

FIG. 1. Mass distributions of K^- (a) and K^+ (b) with the corresponding background fits (dashed lines). (c) Invariant mass distribution of K^+K^- pairs normalized to the number of LVL1 events in $\pi^- + \mathrm{C}$ (pink points) and $\pi^- + \mathrm{W}$ reactions (blue points). The fit to the uncorrected experimental data consists of the sum of two Gaussians for the ϕ signal together with the background described by a polynominal and Gaussian function (dashed line).

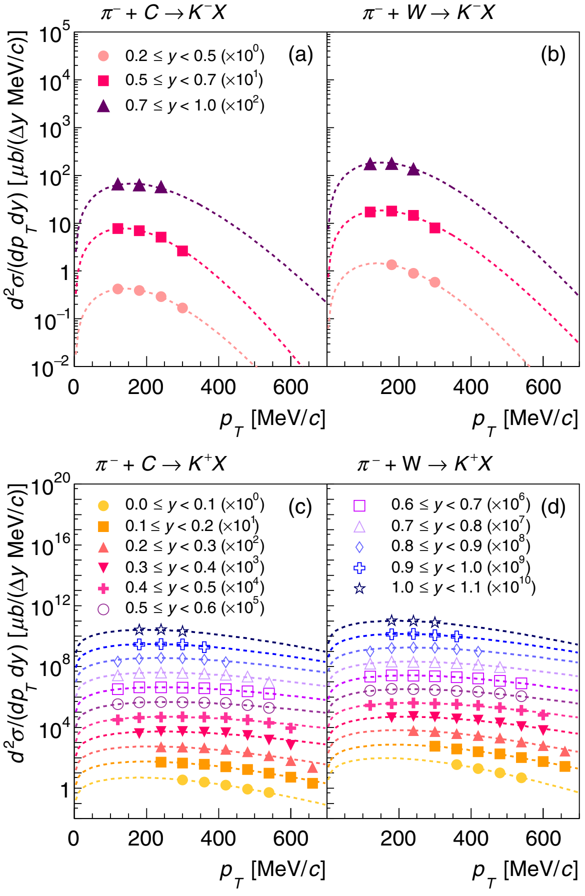

FIG. 2. K^+ and K^- differential cross sections in different rapidity regions (see legend). The upper panel corresponds to K^- and the lower panel to K^+. The combined, statistical and systematic, uncertainty and the normalization error are smaller than the symbol size. The dashed lines indicate Boltzmann fits (see text for details).

Charged kaons were preidentified on the basis of the specific energy loss in the MDC as a function of the momentum [37]. The analyses of the $\pi^- + \mathrm{C}$ and $\pi^- + \mathrm{W}$ reactions were performed in two sets of kinematic variables: $p_T - y$ and $p - \theta$ in the laboratory frame. The (anti) kaon yield was extracted by fitting the measured mass distributions [examples in Figs. 1(a) and 1(b)] obtained for the different $p_T - y$ $(p - \theta)$ intervals [38]. The precision of the kaon mass measurement varies between 3–5% and the resolution between 18.3 to 62.8 MeV/c^2 over the different $p_T - y$ bins. The total number of reconstructed K^+ and K^- for the $p_T - y$ analysis within the HADES acceptance in $\pi^- + \mathrm{C}$ reactions are equal to $N_{\mathrm{C}}^{K^+} = 160\,820 \pm 561$ and $N_{\mathrm{C}}^{K^-} = 7310 \pm 138$, and in $\pi^- + \mathrm{W}$ reactions are equal to $N_{\mathrm{W}}^{K^+} = 208\,783 \pm 602$ and $N_{\mathrm{W}}^{K^-} = 4106 \pm 123$. The obtained double-differential yields of K^+ and K^- were corrected for reconstruction efficiency within the geometrical acceptance ($\approx$12–30% for K^+ and $\approx$10–26% for K^-) and normalized to the total number of beam particles and the density of target atoms to obtain absolute cross sections.

The resulting differential cross sections for K^+ and K^- produced in $\pi^- + \mathrm{C}$ and $\pi^- + \mathrm{W}$ reactions are shown in Fig. 2. Figures 2(a) and 2(b) show the p_T distributions of the K^- in three different rapidity intervals subdividing the range $0.2 \leq y < 1.0$ in $\pi^- + \mathrm{C}$ and $\pi^- + \mathrm{W}$, respectively. Figure 2(c) depicts the p_T distribution of the K^+ in 11 rapidity intervals subdividing the range $0 \leq y < 1.1$. Figure 2(d) shows the analog for the $\pi^- + W$ system. The errors in Fig. 2 are the combined statistical and systematic and normalization uncertainty. The systematic uncertainty was obtained by varying the two-dimensional (anti)kaon identification cut corresponding to (typical) average signal-to-background ratios in $\pi^- + \mathrm{C}$ reactions equal to $S/B_{\mathrm{C}}^{K^+} = 6.8$–$25.8$ and $S/B_{\mathrm{C}}^{K^-} = 4.3$–$9.1$ and in $\pi^- + \mathrm{W}$ reactions equal to $S/B_{\mathrm{W}}^{K^+} = 6.9$–$8.6$ and $S/B_{\mathrm{W}}^{K^-} = 1.8$–$3.1$. Furthermore, the width of the Gaussian function used to fit the experimental (anti)kaon mass distribution is fixed to the maximum allowed limits obtained from simulations [37]. The correction uncertainty corresponds to 3%. The normalization error arises from the beam particle determination and is around 15%.

Following the prescription already adopted in Refs. [39–41], a Boltzmann fit $(d^2N/(dp_T dy) = C(y) p_T \sqrt{p_T^2 + m_0^2} \cdot \exp[-\sqrt{p_T^2 + m_0^2}/T_{\mathrm{B}}(y)]$, where $C(y)$ denotes a scaling factor, m_0 the nominal mass and $T_{\mathrm{B}}(y)$ is the inverse-slope parameter) is applied to the measured p_T spectra and the fit results are shown by the dashed lines in Fig. 2. The fits are used to extrapolate the measured distributions to uncovered transverse momentum regions. The resulting experimental rapidity density distribution for K^+ and K^- are shown in Fig. 3(a). The extrapolation error corresponding to the uncertainty of the Boltzmann fit is the

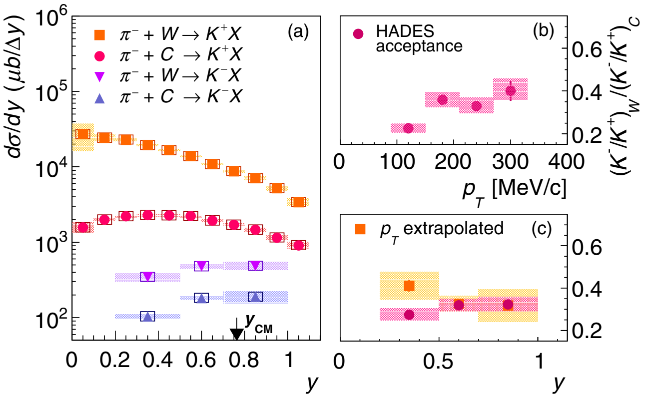

FIG. 3. (a) Cross section of K^+ and K^- in $\pi^- + \mathrm{C}$ and $\pi^- + \mathrm{W}$ collisions as a function of rapidity. The shaded bands denote the systematic errors. The open boxes indicate the normalization error. The statistical uncertainties are smaller than the symbol size. The arrow (y_{CM}) indicates the πN rapidity. Double ratio $(K^-/K^+)_\mathrm{W}/(K^-/K^+)_\mathrm{C}$ as a function of p_T (b) and the rapidity y (c) without (pink circles) and with p_T extrapolation (orange squares) inside the HADES acceptance. The shaded areas indicate the systematic errors.

dominant contribution to the systematic uncertainty. The rapidity distribution for K^+ looks very different for the two colliding systems. (Elastic) scattering shifts the distribution to backward rapidity in the heavier target (W), while charge exchange is negligible [42]. The shape of the K^- rapidity distributions look similar for both nuclear environments, here absorption processes (e.g., $K^-N \to YN$) are dominating. The integrated differential production cross section ($\Delta\sigma$) for K^+ ($0 \le y < 1.1$) and K^- ($0.2 \le y < 1.0$) in $\pi^- + \mathrm{C}$ and $\pi^- + \mathrm{W}$ reactions inside the HADES acceptance are listed in Table I.

In order to study the K^- absorption inside the nuclear medium, a comparison of the K^-/K^+ ratio measured in collisions with the heavy target (W) and the lighter one (C) is carried out. In the double ratio $(K^-/K^+)_\mathrm{W}/(K^-/K^+)_\mathrm{C}$ the K^+ acts as a reference particle for the strange hadron production, because of its very low absorption cross section. Therefore, the measured K^- distribution is normalized to the integrated K^+ yield ($0 \le y < 1.1$).

TABLE I. Target, particle species, and cross section for K^+ ($0 \le y < 1.1$), K^- ($0.2 \le y < 1.0$), and ϕ ($0.4 \le y < 1.0$, $150 \le p_T < 650$ MeV/c). Error values shown are statistic (first), systematic (second), and normalization (third).

Target	Particle	$\Delta\sigma$ [μb]
C	K^+	$1974 \pm 7^{+67}_{-69} \pm 310$
C	K^-	$124 \pm 2 \pm 11 \pm 20$
C	ϕ	$41 \pm 2 \pm 2^{+6}_{-5}$
W	K^+	$15965 \pm 46^{+1236}_{-1247} \pm 2509$
W	K^-	$345 \pm 10 \pm 26 \pm 54$
W	ϕ	$112 \pm 10 \pm 5^{+18}_{-14}$

The double ratio $(K^-/K^+)_\mathrm{W}/(K^-/K^+)_\mathrm{C}$ inside the HADES acceptance is moderately increasing with increasing p_T as shown in Fig. 3(b). Within errors no significant dependence on the rapidity y [Fig. 3(c)], with and without p_T extrapolation, is observed with an average value of $(K^-/K^+)_\mathrm{W}/(K^-/K^+)_\mathrm{C} = 0.319 \pm 0.009(\mathrm{stat})^{+0.014}_{-0.012}(\mathrm{syst})$ in the latter case. In order to define a reference value in which no nuclear absorption is present, a double ratio $(K^-/K^+)_\mathrm{W}/(K^-/K^+)_\mathrm{C}$ was constructed considering $\pi^- N$ reactions and scaling the elementary cross sections by the number of participating nucleons in each target. This procedure results in a value of 0.93 ± 0.09 [38]. The fact that the measured double ratios are well below this reference demonstrates the K^- absorption.

The ϕ mesons were identified via their dominant decay channel into K^+K^- pairs ($BR = 48.9 \pm 0.5\%$ [11]). Both charged kaons were selected by a β vs momentum cut ($p/\sqrt{p^2 + m_0^2} \pm 0.5 \gtrless \beta$, $m_0 = 493.677$ MeV/c^2 [11]). The contamination from other particle species was further reduced by selecting a reconstructed (anti)kaon mass interval of $400 < m < 600$ MeV/c^2. The nominal mass m_0 was attributed to the identified (anti)kaon candidates. The resulting K^+K^- invariant mass distribution for $\pi^- + \mathrm{C}$ and $\pi^- + \mathrm{W}$ collisions normalized to the number of LVL1 events is shown in Fig. 1(c). A clear ϕ peak is visible and the signal can be described by the sum of two Gaussian distributions to account for finite resolution effects as well as for the rescattering of the K^+ and K^- inside the targets. The background is modeled by a third-order polynomial together with a Gaussian to account for the mass threshold ($2 \times m_0$).

The precision of the ϕ mass measurement is better than 1 MeV and the ϕ mass resolutions are 4.0 ± 0.8 MeV/c^2 and 5.5 ± 2.4 MeV/c^2 for C and W targets, respectively. In total $N^\phi_\mathrm{C} = 578 \pm 35$ and $N^\phi_\mathrm{W} = 341 \pm 32$ ϕ mesons are reconstructed. The acceptance and efficiency was determined by simulating the reaction $\pi^- + p(^{12}\mathrm{C}) \to \phi[\to K^+K^-] + n(^{11}\mathrm{B})$ and values of $\approx(2-15)\%$ were obtained. As these corrections strongly depend on the ϕ kinematics, a differential correction as a function of $p_T - y\,(p - \theta)$ was evaluated [43]. Since the limited statistics does not allow for a double differential analysis, each ϕ candidate is weighted with its corresponding correction factor and an integrated K^+K^- invariant mass spectrum is built. The same fitting procedure employed for the uncorrected K^+K^- invariant mass distribution to extract the raw ϕ yields was applied also to the corrected spectra. After the correction for the branching ratio the integrated differential ϕ production cross sections ($\Delta\sigma$) within the HADES acceptance ($0.4 \le y < 1.0$ and $150 \le p_T < 650$ MeV/c) for $\pi^- + \mathrm{C}$ and $\pi^- + \mathrm{W}$ are listed in Table I. The systematic uncertainty was evaluated by varying the invariant mass binning with respect to the standard analysis as well as by changing the order of the polynominal used to fit the background from third to second order. The correction uncertainty corresponds to 3% for each kaon.

The ϕ absorption can be quantified in terms of the transparency ratio defined as $T = [(12/184)(\Delta\sigma^{\phi}_{\mathrm{W}}/\Delta\sigma^{\phi}_{\mathrm{C}})]$. This value is equal to $0.18 \pm 0.02(\mathrm{stat}) \pm 0.01(\mathrm{syst})^{+0.04}_{-0.03}(\mathrm{norm})$ and hence smaller than the results obtained in $p + A$ by ANKE [44] and $\gamma + A$ by CLAS [45] for slightly bigger nuclei [$T_{\mathrm{ANKE}} = 0.29 \pm 0.01(\mathrm{stat}) \pm 0.02(\mathrm{syst})$, $T_{\mathrm{CLAS}} = 0.46 \pm 0.12(\mathrm{stat}) \pm 0.13(\mathrm{syst})$]. The lower transparency ratio found in pion-induced reactions may be attributed to the already mentioned large πN reaction cross section and the negligible contribution of secondary reactions that lead to ϕ production near the upstream surface, allowing the hadron to travel a longer path within the nucleus than in proton- and photon-induced reactions.

The ϕ/K^- ratio was evaluated for both collision systems inside the HADES acceptance. For this investigation it has to be considered that the K^- and ϕ phase space coverage of HADES is different ($0.4 \leq y_{\phi} < 1$ and $0.2 \leq y_{K^-} < 1$, $150 \leq p_{T,\phi} < 650\ \mathrm{MeV}/c$, and $90 \leq p_{T,K^-} < 330\ \mathrm{MeV}/c$). As shown in Fig. 3(a) the shape of the K^- rapidity distributions does not depend on the target. To demonstrate that also the ϕ distributions share the same feature, GIBUU [46] simulations were carried out for the $\pi^- + \mathrm{C(W)}$ systems and no bias due to the HADES geometrical acceptance was found.

The measured ϕ/K^- ratio within the HADES acceptance is $0.55 \pm 0.04(\mathrm{stat})^{+0.06}_{-0.07}(\mathrm{syst})$ for $\pi^- + \mathrm{C}$ and $0.63 \pm 0.06(\mathrm{stat})^{+0.11}_{-0.11}(\mathrm{syst})$ for $\pi^- + \mathrm{W}$ collisions. The main systematic error arises from the difference in the $p_T - y$ and $p - \theta$ analyses. Within errors the two ϕ/K^- ratios are in agreement. Since the double ratio $(K^-/K^+)_{\mathrm{W}}/(K^-/K^+)_{\mathrm{C}}$ [Fig. 3(b)] clearly indicates a larger K^- absorption in the W target and since the ϕ/K^- ratios are the same for both targets, also a stronger ϕ absorption in W is observed. This demonstrates that both resonant and nonresonant channels are affected in the medium in the same way.

In summary, the inclusive production cross sections of charged kaons and ϕ mesons in $\pi^- + A$ collisions within the HADES acceptance were measured. The rapidity density distributions for K^+ and K^- produced on heavy (W) and light (C) nuclei were compared. Strong scattering effects are observed shifting the maximum of the K^+ distribution to backward rapidity in the heavier target, while the shape of the K^- distribution is comparable in both targets. The measured double ratio $(K^-/K^+)_{\mathrm{W}}/(K^-/K^+)_{\mathrm{C}}$ given in Table II is well below the expected (anti)kaon production reference based on elementary πN reactions, directly indicating sizable K^- absorption in heavy nuclei (W) with respect to light ones (C). The ϕ/K^- ratios for $\pi^- + \mathrm{C}$ and $\pi^- + \mathrm{W}$ reactions within the HADES acceptance listed in Table II are consistent within the uncertainties pointing to a non-negligible ϕ absorption. This finding is in line with the extracted ϕ transparency ratio of ≈18%, which is lower than observed by ANKE [44] and CLAS [45] measurements. This first measurement of kaons and ϕ in the same reactions provides experimental evidence of the strong coupling between the ϕ and K^- dynamics within nuclear matter with direct consequences for an improved description of heavy-ion collisions and the equation of state of neutron stars.

TABLE II. Particle ratios inside the HADES acceptance (see text for details). Error values shown are statistic (first), systematic (second), and normalization (third).

Ratios	
$(K^-/K^+)_{\mathrm{W}}/(K^-/K^+)_{\mathrm{C}}$	$0.319 \pm 0.009^{+0.014}_{-0.012}$
$(\phi/K^-)_{\mathrm{C}}$	$0.55 \pm 0.04^{+0.06}_{-0.07}$
$(\phi/K^-)_{\mathrm{W}}$	$0.63 \pm 0.06 \pm 0.11$
$T = [(12/184)(\Delta\sigma^{\phi}_{\mathrm{W}}/\Delta\sigma^{\phi}_{\mathrm{C}})]$	$0.18 \pm 0.02 \pm 0.01^{+0.04}_{-0.03}$

The HADES Collaboration gratefully acknowledges the support given by the following institutions and agencies: SIP JUC Cracow, Cracow (Poland), National Science Center 2016/23/P/ST2/040 POLONEZ, 2017/26/M/ST2/00600, 2017/25/N/ST2/00580; TU Darmstadt, Darmstadt (Germany) and Goethe-University, Frankfurt (Germany), ExtreMe Matter Institute EMMI at GSI Darmstadt; TU München, Garching (Germany), MLL München, DFG EClust 153, GSI TMLRG1316F, BmBF 05P15WOFCA, SFB 1258, DFG FAB898/2-2; NRNU MEPhI Moscow, Moscow (Russia), in framework of Russian Academic Excellence Project 02.a03.21.0005, Ministry of Science and Education of the Russian Federation 3.3380.2017/4.6; JLU Giessen, Giessen (Germany), BMBF:05P12RGGHM; IPN Orsay, Orsay Cedex (France), CNRS/IN2P3; and NPI CAS, Rez, Rez (Czech Republic), MSMT LM2015049, OP VVV CZ.02.1.01/0.0/0.0/16 013/0001677, LTT17003.

---

[*] Deceased.

[a] Also at Coimbra Polytechnic—ISEC, Coimbra, Portugal.

[b] Also at ExtreMe Matter Institute EMMI, 64291 Darmstadt, Germany.

[c] Also at Technische Universität Dresden, 01062 Dresden, Germany.

[d] Also at Frederick University, 1036 Nicosia, Cyprus.

[e] Corresponding author.
hades-info@gsi.de

[1] N. Kaiser, P. B. Siegel, and W. Weise, Nucl. Phys. **A594**, 325 (1995).

[2] E. Oset and A. Ramos, Nucl. Phys. **A635**, 99 (1998).

[3] C. Fuchs, Prog. Part. Nucl. Phys. **56**, 1 (2006).

[4] J. A. Oller and U. G. Meissner, Phys. Lett. B **500**, 263 (2001).

[5] Y. Ikeda, T. Hyodo, and W. Weise, Nucl. Phys. **A881**, 98 (2012).

[6] O. Vázquez Doce *et al.*, Phys. Lett. B **758**, 134 (2016).

[7] K. Piscicchia, S. Wycech, and C. Curceanu, Nucl. Phys. **A954**, 75 (2016).

[8] K. Piscicchia *et al.*, Phys. Lett. B **782**, 339 (2018).

[9] M. Agnello *et al.* (FINUDA Collaboration), Phys. Rev. C **92**, 045204 (2015).

[10] D. Jido, J. A. Oller, E. Oset, A. Ramos, and U. G. Meissner, Nucl. Phys. **A755**, 669 (2005).

[11] C. Patrignani *et al.* (Particle Data Group), Chin. Phys. C **40**, 100001 (2016).

[12] M. Bazzi *et al.* (SIDDHARTA Collaboration), Phys. Lett. B **704**, 113 (2011).

[13] M. Bazzi *et al.* (SIDDHARTA Collaboration), Phys. Lett. B **681**, 310 (2009).

[14] M. Bazzi *et al.* (SIDDHARTA Collaboration), Phys. Lett. B **697**, 199 (2011).

[15] S. Ajimura *et al.* (J-PAC E15 Collaboration), Phys. Lett. B **789**, 620 (2019).

[16] G. E. Brown, V. Thorsson, K. Kubodera, and M. Rho, Phys. Lett. B **291**, 355 (1992).

[17] A. Ramos, J. Schaffner-Bielich, and J. Wambach, Lect. Notes Phys. **578**, 175 (2001).

[18] M. Hanauske, K. Takami, L. Bovard, L. Rezzolla, J. A. Font, F. Galeazzi, and H. Stöcker, Phys. Rev. D **96**, 043004 (2017).

[19] J. Adamczewski-Musch *et al.* (HADES Collaboration), Nat. Phys. (to be published).

[20] P. Gubler and W. Weise, Phys. Lett. B **751**, 396 (2015).

[21] D. Cabrera, A. N. Hiller Blin, and M. J. Vicente Vacas, Phys. Rev. C **95**, 015201 (2017).

[22] B. B. Abelev *et al.* (ALICE Collaboration), Phys. Rev. C **91**, 024609 (2015).

[23] M. Wada (STAR Collaboration), Nucl. Phys. **A904-905**, 1019c (2013).

[24] J. Steinheimer and M. Bleicher, J. Phys. G **43**, 015104 (2016).

[25] S. Okubo, Phys. Rev. D **16**, 2336 (1977); G. Zweig, Report No. CERN-TH-412, 80, 1964, version 1 is CERN preprint8182/TH.401, 1964; J. Iizuka, Prog. Theor. Phys. Suppl. **37–38**, 21 (1966).

[26] M. Hartmann *et al.* (ANKE Collaboration), Phys. Rev. C **85**, 035206 (2012).

[27] T. Ishikawa *et al.* (LEPS@Spring8 Collaboration), Phys. Lett. B **608**, 215 (2005).

[28] R. Muto *et al.* (KEK-PS-E325 Collaboration), Phys. Rev. Lett. **98**, 042501 (2007).

[29] P. Mühlich and U. Mosel, Nucl. Phys. **A765**, 188 (2006).

[30] D. Cabrera, A. N. Hiller Blin, M. J. Vicente Vacas, and P. Fernández de Córdoba, Phys. Rev. C **96**, 034618 (2017).

[31] S. Weissenborn, D. Chatterjee, and J. Schaffner-Bielich, Nucl. Phys. **A881**, 62 (2012).

[32] H. Dapo, B.-J. Schaefer, and J. Wambach, Phys. Rev. C **81**, 035803 (2010).

[33] B. W. Allardyce *et al.*, Nucl. Phys. **A209**, 1 (1973).

[34] M. Benabderrahmane *et al.* (FOPI Collaboration), Phys. Rev. Lett. **102**, 182501 (2009).

[35] G. Agakishiev *et al.* (HADES Collaboration), Eur. Phys. J. A **41**, 243 (2009).

[36] J. Adamczewski-Musch *et al.* (HADES Collaboration), Eur. Phys. J. A **53**, 188 (2017).

[37] J. Wirth (HADES Collaboration), Proc. Sci. BORMIO2017 (**2017**) 011.

[38] J. Wirth (HADES Collaboration), EPJ Web Conf. **171**, 13002 (2018).

[39] G. Agakishiev *et al.* (HADES Collaboration), Phys. Rev. C **88**, 024904 (2013).

[40] G. Agakishiev *et al.* (HADES Collaboration), Eur. Phys. J. A **50**, 81 (2014).

[41] J. Adamczewski-Musch *et al.* (HADES Collaboration), Phys. Lett. B **781**, 735 (2018).

[42] C. J. S. Damerell *et al.*, Nucl. Phys. **B94**, 374 (1975).

[43] J. Wirth (HADES Collaboration), EPJ Web Conf. **181**, 01010 (2018).

[44] A. Polyanskiy *et al.* (ANKE Collaboration), Phys. Lett. B **695**, 74 (2011).

[45] M. H. Wood *et al.* (CLAS Collaboration), Phys. Rev. Lett. **105**, 112301 (2010).

[46] O. Buss, T. Gaitanos, K. Gallmeister, H. van Hees, M. Kaskulov, O. Lalakulich, A. Larionov, T. Leitner, J. Weil, and U. Mosel, Phys. Rep. **512**, 1 (2012).